5.4. Amundsen-Scott South Pole Station

The South Pole system is installed at the top of the recently completed Atmospheric Research Observatory (ARO, shown) at Amundsen-Scott South Pole Station, located at the geographical South Pole. This system operates in one of the harshest environments on the planet, with average temperatures of -49°C. This advantageous location provides data that are virtually free of daily changes in solar zenith angle, at substantial elevation (approx. 2841 M), in the cleanest known atmospheric environment on Earth.

Prior to 1991, the instrument was located on top of the former Clean Air Facility (CAF). Access was allowed only from outside the facility. From January 1991 to January 1997, the instrument was built into an enclosure of the CAF allowing access from within the laboratory. In January 1997 the system was relocated from the CAF to ARO into a specially built "penthouse" room at the ARO.

The ARO is visited regularly by ASA/NSF personnel. Installation of an improved system control computer in 1997, including new system control software, allows for data transfers and system monitoring to be performed remotely from the main dome-shaped building by the site operator. Data transfers and system monitoring, via direct FTP, are also possible from San Diego, limited only by satellite availability.

As at the other facilities, data are recorded onto both a 120-MB removable hard disk media and a hard disk drive internal to the system control computer. In addition to the system control computer, a second PC is used as a backup spare, and to transmit data over the Internet directly to BSI.

The South Pole is normally accessible only by airplane between November and February. Prior to the facility upgrade in 1991, the instrument was only successfully operated on an occasional basis.

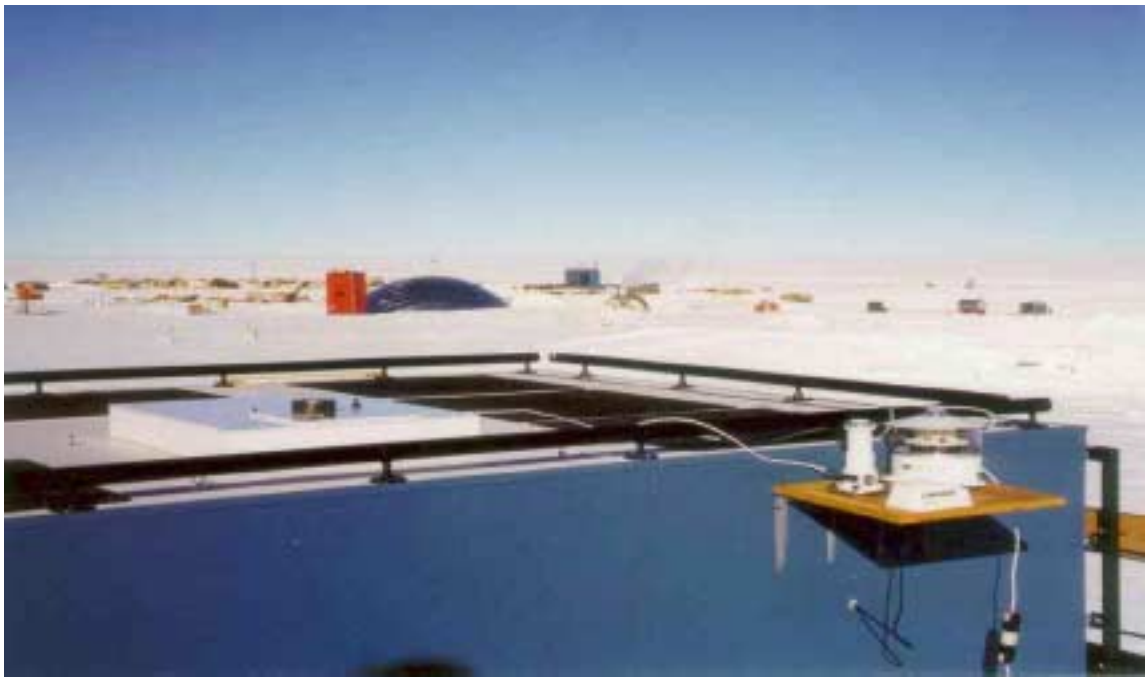

Figure 5.4.1. *The instrument is installed at the top of the Atmospheric Research Observatory (ARO), completed in 1997, at Amundsen-Scott South Pole Station.*

Table 5.4.1 Objects in the collector's field-of-view at the South Pole.

Object	Bearing	Elevation
Open frame radio tower	334.00° - 335.30°	7.83°
Galvanized steel wrapped exhaust stack	87.61° - 89.60°	15.26°
Galvanized steel wrapped exhaust stack	91.56° - 93.56°	17.21°
Open frame radio tower	181.89°	1.94°
Open frame radio tower with "T" shape construction at top, having a horizontal angular width of 2.25°	198.31° - 199.60°	1.39°

Notes: Sightings were made in January 1998 by ASA Surveying staff. Bearings are relative to the Grid North.

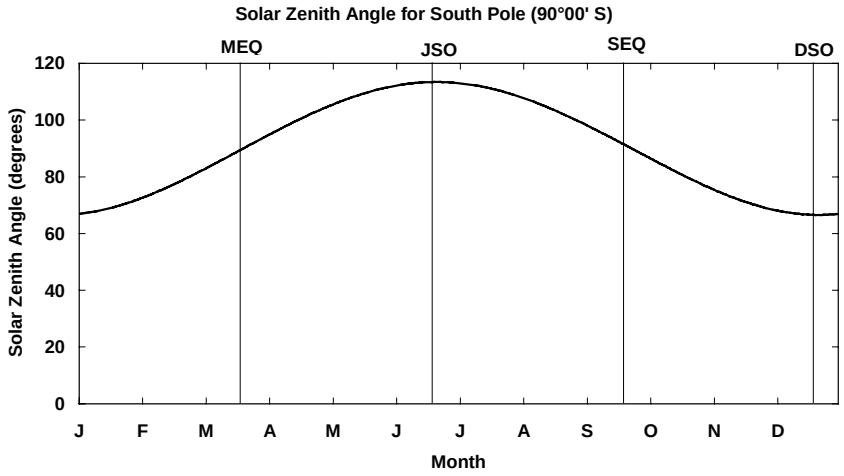

Figure 5.4.2.

Plot of noontime solar zenith angle at South Pole. (MEQ = March equinox, JSO = June solstice, SEQ = September equinox, DSO = December solstice).

5.4.1 Weather Observations

Weather observations for South Pole Station (WMO station number 89009) were obtained from the National Climatic Data Center (NCDC). The data are in a format described in Appendix A7 of this report. This file, SOUTHPOLE.CSV, can be found in the \WEATHER directory on the CD-ROM 7.0.b.

5.4.2. Ozone Observations

Table 5.4.2 TOMS ozone averages and minima for South Pole, September 27 – December 31.

	TOMS												TOVS		
	Nimbus 7			Meteor 3			Adeos			Earth Probe					
Year	Avg	Min	Date	Avg	Min	Date	Avg	Min	Date	Avg	Min	Date	Avg	Min	Date
1988	310.7	187	10/11/88												
1989	240.4	135	10/10/89												
1990	207.9	130	10/5/90												
1991	253.7	111	10/5/91	258.4	128	10/6/91									
1992	213.2	131	10/12/92	214.8	120	10/11/92									
1993				205.4	89	10/8/93, 10/12/93									
1994				206.34	108	10/2/94							231.9	93	10/23/94
1995													185.3	102	10/18/95
1996							216.3	108	9/30/96	220.0	112	10/5/96	178.3	105	10/25/96
1997										215.7	117	10/07/97			
1998										167.7	105	10/06/98			

Note: Earth Probe data from the years 1996, 1997, and 1998 is only available for the period 1-Oct – 31-Dec.

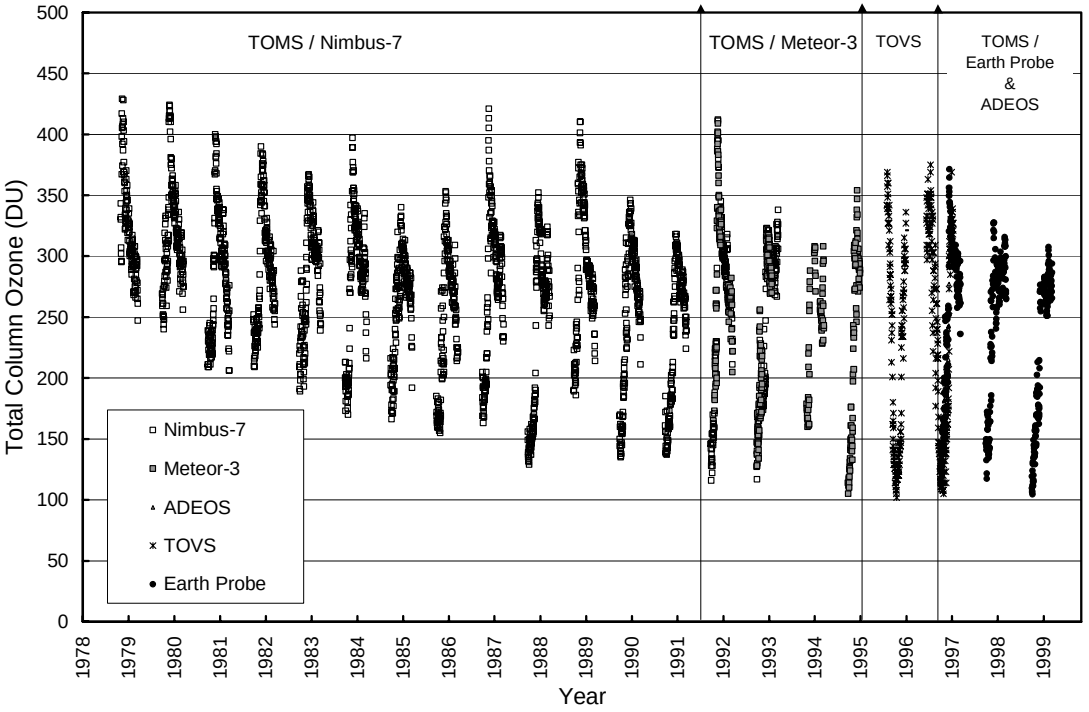

Figure 5.4.3. *Total ozone column time series from TOMS at the South Pole. In recent years, ozone values in October dropped down to about 100 DU.*

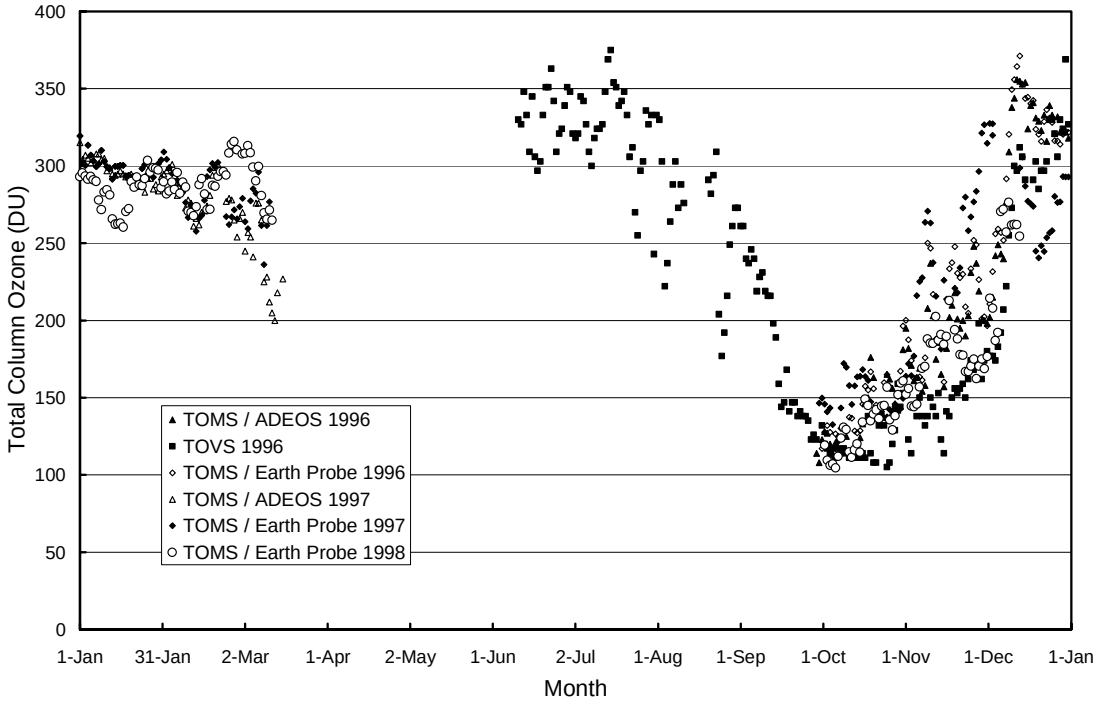

Figure 5.4.4. *Seasonal trends in ozone from TOMS and TOVS. In contrast to TOMS, TOVS ozone measurements do not require backscattered sunlight. Therefore only TOVS data is available during austral winter indicating the lowest ozone concentration in early October.*

5.4.3. South Pole 1/16/97 - 1/8/98

The 1997/98 season at South Pole is defined as the time between the site visits 01/16/97 – 01/31/97 and 01/04/98 – 01/08/98. The season opening and closing calibrations were performed on 1/27/97 and 1/4/98, respectively. Solar data is available for the period 2/1/97 – 1/3/98. The site visit in 1997 was comparatively long because the system had to be relocated from the old Clean Air Facility (CAF) to the new Atmospheric Research Observatory (ARO). The stability of the response lamp was very good during the entire period. Overall system performance in 1997, however, was affected by several problems, causing both a reduced accuracy and gaps in the data. Some of these problems were introduced by system relocation:

- Because of an incorrect PMT offset, data at short wavelengths have a reduced accuracy between the season start and day 10/15/97. The problem is described below in detail.

- It appears that the system's optics block consisting of diffuser, response lamp, wavelength standard, and beam splitters became misaligned during the relocation of the system. This increased the azimuth dependency of the system. This means that measurements of solar irradiance depend on the azimuth position of the Sun. Since the solar zenith angle at South Pole is fairly constant during a day, the azimuth dependence appears as a sinusoidal wiggle in the data with a periodicity of one day. Examples of this effect are given below.

- Due to a hard disk failure no data is available during 2/10/97 and 2/20/97.

The calibration of previous seasons was primarily based on a 200-Watt Standard of Spectral Irradiance, which had been calibrated by Optronics Laboratories in 1992. The standard appears to have drifted over time and therefore a new calibration was applied to the lamp for the Volume 7 data (see Section 5.4.3.4). The 1992 calibration and the new calibration deviate by approximately 4%, almost independent of wavelength. Time series of solar data including Volumes 6 and 7 are affected by this change in the calibration scale, but to a lesser extent (i.e., 2%) because calibrations are not based solely on this lamp.

5.4.3.1. South Pole Volume 7 Offset Problem

The system module that digitizes the PMT anode can only handle positive currents. In order to assure that the module's input current is always positive, an electronic offset is artificially applied to the PMT-signal at all sites. As described in Section 3, the sum $I_{dark}(V)$ of the actual PMT-dark current and this artificial offset is automatically measured during each data scan. To calculate solar irradiance, $I_{dark}(V)$ is subtracted from the PMT-signal $I_{solar}(V)$ (see Section 3):

$$E_{solar}(\lambda) = \frac{I_{solar}(\lambda,V) - I_{dark}(V)}{R(\lambda,V)}$$

Unfortunately, the digitizing module did not function after the relocation of the South Pole system and had to be replaced. The artificial offset of the spare was negative until the electronics were fixed on 10/15/97. During the period between start of the season and 10/15/97, negative PMT-currents were therefore digitized as "zero." The problem mostly affects measurements at short wavelengths where the signal is low. The cutoff-wavelength was approximately 303 nm. Measurements below this wavelength cannot be corrected and data at short wavelengths are therefore not available.

Above the cutoff-wavelength, solar irradiance was calculated with the formula given above. Data have a higher uncertainty, however, because $I_{dark}(V)$ could not be determined from Items 1 and 4 of the data scan, as is usually done (see Section 3 for details). $I_{dark}(V)$ was instead estimated from Items 2 and 5 of several absolute scans. These items include the PMT current when measuring a 200 W lamp at two different high voltages. If $I_{dark}(V)$ were zero for both items, the ratio would be nearly independent of wavelength. If $I_{dark}(V)$ does not equal zero, which is the usual case, the ratio becomes wavelength dependent. $I_{dark}(V)$ was finally derived from this characteristic dependency.

The indirect estimate of $I_{dark}(V)$ leads to a higher uncertainty, depending mainly on the signal level. The uncertainty is therefore highest at high solar zenith angle and short wavelengths. For the time-period between the end of Polar Night and the date problem was fixed (10/14/97), the following uncertainties (±2σ) apply:

- 85° SZA, 305 nm: ±1%
- 85° SZA, 310 nm: < ± 0.5%
- 88° SZA, 305 nm: ±6%
- 88° SZA, 310 nm: ± 1.5%

Since the cutoff-wavelength is about 303 nm, dose weightings are strongly affected by the offset problem. For example, the product of solar spectral irradiance and the DNA-weighting function peaks at about 306 nm. The contribution of solar spectral irradiance with wavelengths below 303 nm is therefore not negligible when calculating DNA weighted dose with the integral

$$E_{\text{bio}} = \int_{\lambda_1}^{\lambda_2} E(\lambda) W(\lambda)\, d\lambda$$

We therefore decided not to publish dose weightings (except erythemally (CIE) weighted dose 3) for the period that is affected.

5.4.3.2. Stability in the Wavelength Domain

As for the other sites, wavelength stability of the system was monitored with the internal Mercury lamp. Information from the daily wavelength scans was used to homogenize the data set by correcting day-to-day fluctuations of the wavelength offset. After this step, there may still be a deviation from the correct wavelength scale but this bias should ideally be the same for all days. Figure 5.4.5 shows the differences in the wavelength offset of the 296.73-nm mercury line between two consecutive wavelength scans. In total, 277 scans were evaluated. For 72% of the days, the change in offset is smaller than ±0.025 nm; for 95% of the days the shift is smaller than ±0.055 nm. For 9 scans (3.25%) the offset-difference is larger than ± 0.1 nm. The reasons for these deviations were carefully examined, see Table 5.4.3. Whenever a change in the wavelength alignment of the monochromator occurred, great care was taken that no data scan was incorrectly adjusted with a wavelength scan taken before or after the change of the wavelength scale.

Table 5.4.3. Worst case wavelength differences between consecutive scans.

First Wavelength File	Second Wavelength File	First Date	Second Date	Wavelength shift Second-First	Cause
CM971100.034	CW970653.037	2/3/97	2/6/97	-4.185	Wavelength position reset
CW970653.037	CM971100.037	2/6/97	2/6/97	4.503	Wavelength adjusted
CM971800.065	CM970329.071	3/6/97	3/12/97	1.467	Wavelength position manually adjusted
CM970329.071	CM971100.071	3/12/97	3/12/97	-1.419	Wavelength position manually adjusted
CM971030.174	CM971030.179	6/23/97	6/28/97	-0.400	System reset
CW970617.190	CM971030.191	7/9/97	7/10/97	0.444	Wavelength position manually adjusted
CM971030.209	CM971030.211	7/28/97	7/30/97	0.352	Unknown
CM971045.283	CM971045.289	10/10/97	10/16/97	1.857	System reset
CM971045.295	CM971045.296	10/22/97	10/23/97	-2.219	Wavelength position manually adjusted

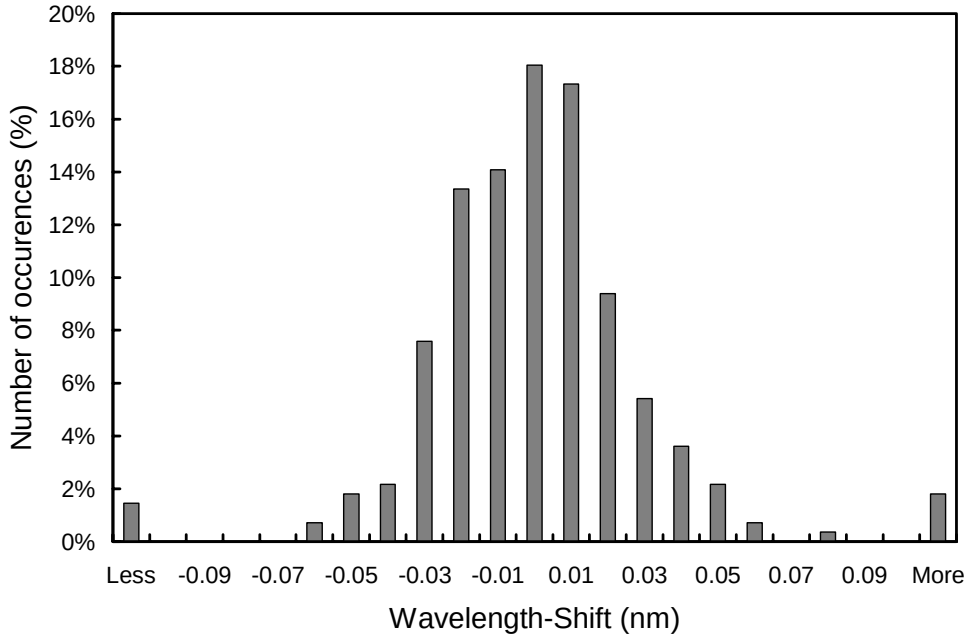

Figure 5.4.5. *Differences in the measured position of the 296.72 nm Mercury line between consecutive wavelength scans. The x-labels give the center wavelength shift for each column. Thus the 0-nm histogram column covers the range -0.005 to +0.005 nm. "Less" means shifts smaller than –0.105 nm; "more" means shifts larger than 0.105 nm.*

After the data was corrected for day-to-day wavelength fluctuations, the wavelength-dependent bias between this homogenized data set and the correct wavelength scale was determined with the Fraunhofer-correlation method, as described in Section 3. The thick line in Figure 5.4.6 shows the resulting correction function that was applied to the Volume 7 South Pole data. The function clearly depends on wavelength. This is caused by non-linearities of the monochromator drive. In order to demonstrate the difference between the result of the new Fraunhofer-correlation method and the method that was historically applied, Figure 5.4.6 also includes a correction function that was calculated with the "old" method, i.e., the function is based on internal wavelength scans only. The average difference between both approaches is about 0.074 nm. As explained in Section 3, this bias is caused by the different light paths for internal wavelength scans and solar measurements.

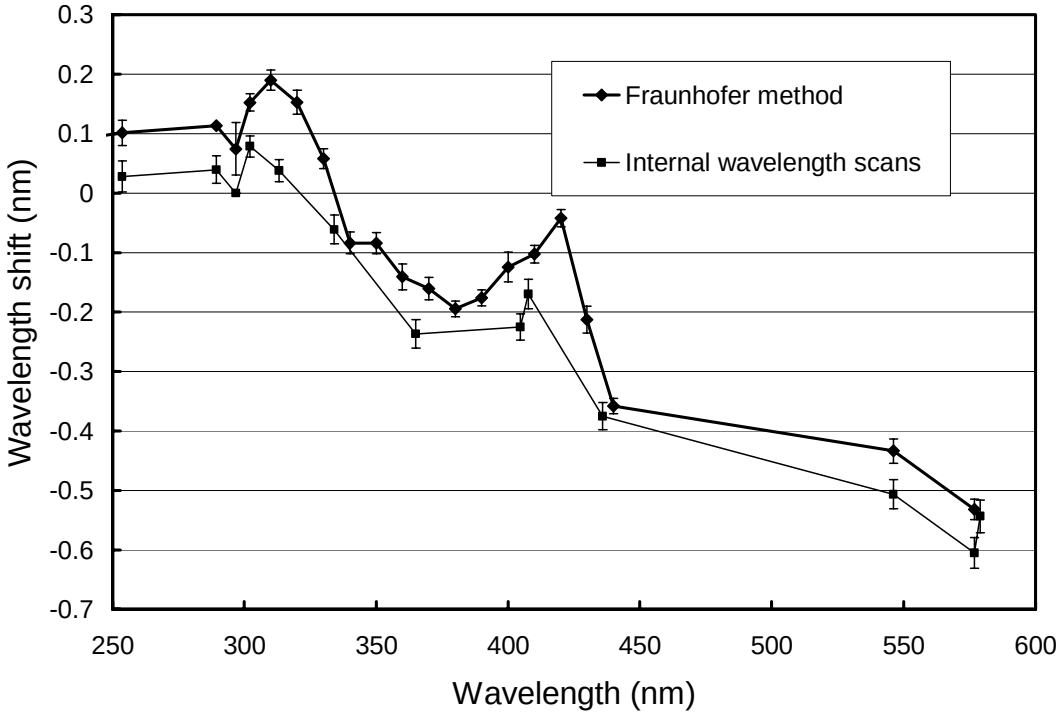

Figure 5.4.6. *Functions expressing the monochromator non-linearity for South Pole. Thick line: Function calculated with the Fraunhofer-correlation method. This function was applied to correct the South Pole Volume 7 data. Thin line: Function calculated with the method that was historically applied. The offset between both methods is approximately 0.074 nm. Both functions represent average wavelength shifts for the 1997/98 season. The error bars give the 1σ standard deviation variation of the wavelength shifts of individual days.*

After the data was wavelength corrected using the shift-function described above, the wavelength accuracy was tested again with the Fraunhofer method. The result is shown in Figure 5.4.7. The plot is divided in two periods, one before and one after Polar Night. In austral spring (after Polar Night) wavelength shifts for noontime measurements are smaller than ±0.05 nm both at 310 nm and 350 nm. Immediately after the season opening site visit the residual shift was somewhat larger for both wavelengths. The scatter in the 310 nm values in late March 1997 is also higher because during this part of the year the solar zenith angle is already larger than 85°. At these angles, the irradiance at 310 nm is rather low and an accurate application of the correlation method is not possible. High shift values indicate therefore a problem in the correlation algorithm rather than an actual wavelength shift of the monochromator. The actual wavelength uncertainty may be a little larger than the shifts shown in Figure 5.4.7 because of possible systematic errors of the Fraunhofer correlation method (see Section 3). The shifts for other wavelengths in the UV have a very similar pattern to the shifts presented in Figure 5.4.7.

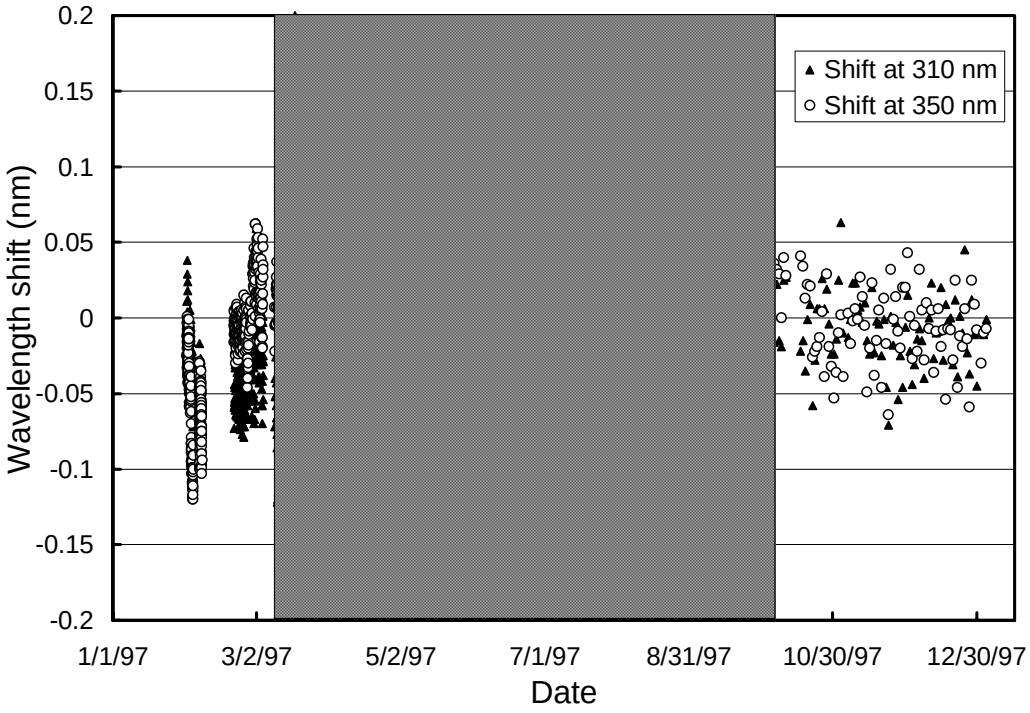

Figure 5.4.7. *Check of the wavelength accuracy of the final data by means of Fraunhofer correlation. She shaded area marks the days during Polar Night when the solar zenith angle is larger than 85°. For days before Polar Night shift values were determined for each spectrum; after Polar Night (in the austral spring) the shift values were determined for noontime spectra only, as for the other sites. During austral spring, the shifts fluctuate randomly between about -0.05 nm and +0.05 nm. The shifts are somewhat larger immediately after the season opening in February 1997. The scatter in the 310 nm values in late March 1997 is also higher because during this part of the year the solar zenith angle is already larger than 85°. At these angles, the irradiance at 310 nm is rather low and an accurate application of the correlation method is not possible.The gap in the data in mid-February is caused by data loss due to a hard-disk failure.*

Although data from the external mercury scans do not have a direct influence on the data products, they are an important part of the instrument characterization. Figure 5.4.8 illustrates the difference between internal and external mercury scans collected during both site visits. External scans have a bandwidth of about 1.12 nm FWHM, whereas the bandwidth of the internal scan is only 0.79 nm. In addition, the peak of external scans is shifted towards longer wavelengths compared to the internal peak. Since external scans have the same light path as solar measurements, they more realistically represent the bandpass of the monochromator. The difference in the center wavelength of both scan types is about 0.16 nm. The scans at the start and end of the season are very consistent, as can be seen from Figure 5.4.8.

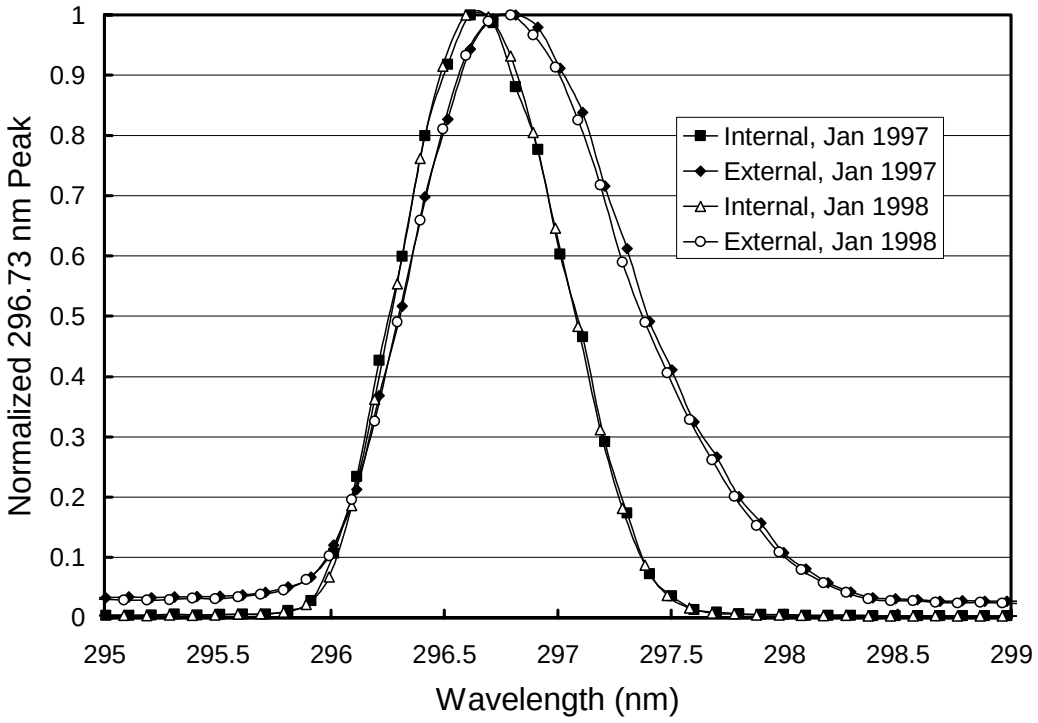

Figure 5.4.8. *The 296.73 mercury line as registered by the PMT from external and internal sources. For this plot, the wavelength calibration is based on the internal scans and it was assumed that the wavelength registration of the monochromator did not shift between internal and external scans, which were close in time.*

5.4.3.3. Responsivity Stability

The stability of the spectroradiometer's responsivity over time is monitored with the internal response lamp. This lamp is also subject to change, however, and it is therefore important to also assess the stability of the lamp.

Instrument and response lamp stability of the Volume 7 South Pole data were primarily assessed using four parameters:

- Total Scene Irradiance (TSI) during response lamp scans
- Photomultiplier Tube (PMT) current at several wavelengths
- Current supplied to the lamp
- Calibrations with 200-W standards

Note that the TSI sensor is completely independent from possible monochromator and PMT drifts, whereas the PMT current is affected by all system parts, including response lamp, monochromator, and PMT, and is also sensitive to temperature changes and high voltage applied. PMT current therefore also provides valuable insight into possible drifts of these components.

Figure 5.4.9 demonstrates that the TSI readings during response lamp scans were stable to within ±1% during the whole 1997/98 South Pole season. The PMT currents at 300 and 400 nm when measuring the response lamp, however, were stable until only mid-September. After this date, the currents steadily increased and were about 25% higher at the end of the season than during Polar Night. Since the TSI measurements were stable during the whole period, this indicates that the instrument became more sensitive during the last months of the season. The reason for this gain is unknown. The increase in instrument

responsivity was further confirmed by using the biweekly calibrations with 200-Watt irradiance standards (circles in Figure 5.4.9). The increase in the PMT current when measuring the 200-Watt standard was very consistent with the change in the current when the response was energized, confirming the gain in sensitivity.

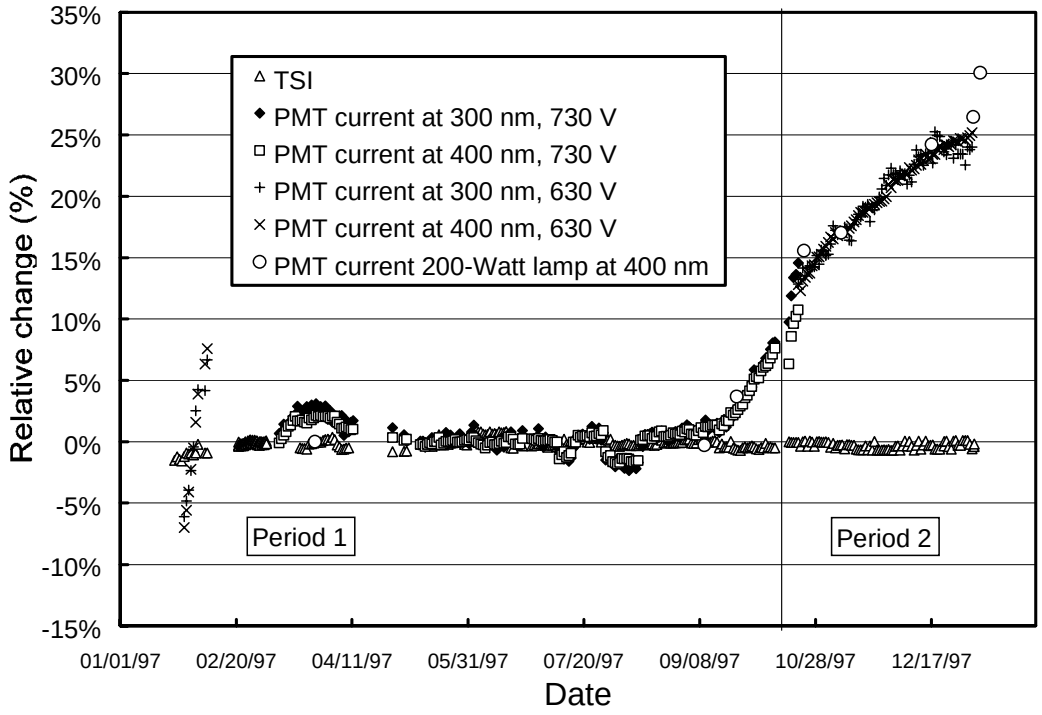

Figure 5.4.9. *Time series of TSI signal during measurements of the response lamp (triangles) and PMT currents at 300 and 400 nm during the South Pole 1997/98 season. The data marked with a circle reflect PMT current at 400 nm during measurements of the 200-Watt standard 200W006. All other PMT currents were recorded when the response lamp was energized. The data is normalized to the average of the measurements between 5/11/97 and 9/13/97. Response lamp measurements at the same high voltage are not available throughout the year. Since PMT currents at 630 V high-voltage are lower than measurements at 730 V, the former were scaled such that the transition between both data series (on 10/20/97) is steady. The season is broken in two periods: Period 1 is affected by the offset problem (see Section 5.4.3.1). Period 2 begins after the problem was fixed.*

Although the instrument's sensitivity drifted significantly the impact on solar data is very small because solar measurements of a given day are always referred to a response lamp scan of that day. The change in sensitivity from day to day never exceeded 2.5% and was usually below 1%. The uncertainty due to the drift is therefore less than ±1%, except on a few occasions.

Since the TSI reading was very stable throughout the year, it would have been appropriate to assign the same mean-irradiance of the response lamp to the whole season (see Section 3 for definition of "mean-irradiance of the response lamp"). We decided, however, to break the season in two parts. Period 1 encompasses the period with the offset problem (see Section 5.4.3.1). In Period 2, the instrument offset was determined correctly.

The "mean-irradiance" that was assigned to the response lamp in Period 1 was calculated from eight 200-Watt lamp calibrations that were carried out in this period. From each of these calibrations, irradiance values for the response lamp were calculated and the mean irradiance was derived by averaging over the individual calibration functions. The same procedure was applied to Period 2, which was also based on

eight calibration spectra. The ratio of the standard deviation, calculated from the calibration functions, and the mean-irradiance, is a useful tool for estimating the variability of the calibrations during each period. Figure 5.4.10 shows that the standard deviation is less than 2% of the average for both periods, except for Period 1 below 300 nm. As detailed in Section 5.4.3.1, spectral solar irradiance data with wavelengths below 305 nm cannot be published for Period 1 because of a negative electronic offset. Thus the calibrations in both periods are consistent at the ±2% (±1σ) level for all wavelengths where data is available.

Figure 5.4.11 shows the difference between the response lamp's mean-irradiances applied in Periods 1 and 2. For wavelengths larger than 300 nm, the mean irradiance for Period 2 is about 2% lower than for Period 1. The increase towards shorter wavelengths is caused by the offset problem, which also affected absolute scans. For the same reason as mentioned above, this offset problem does not affect solar data, which are available from 305 nm onwards only.

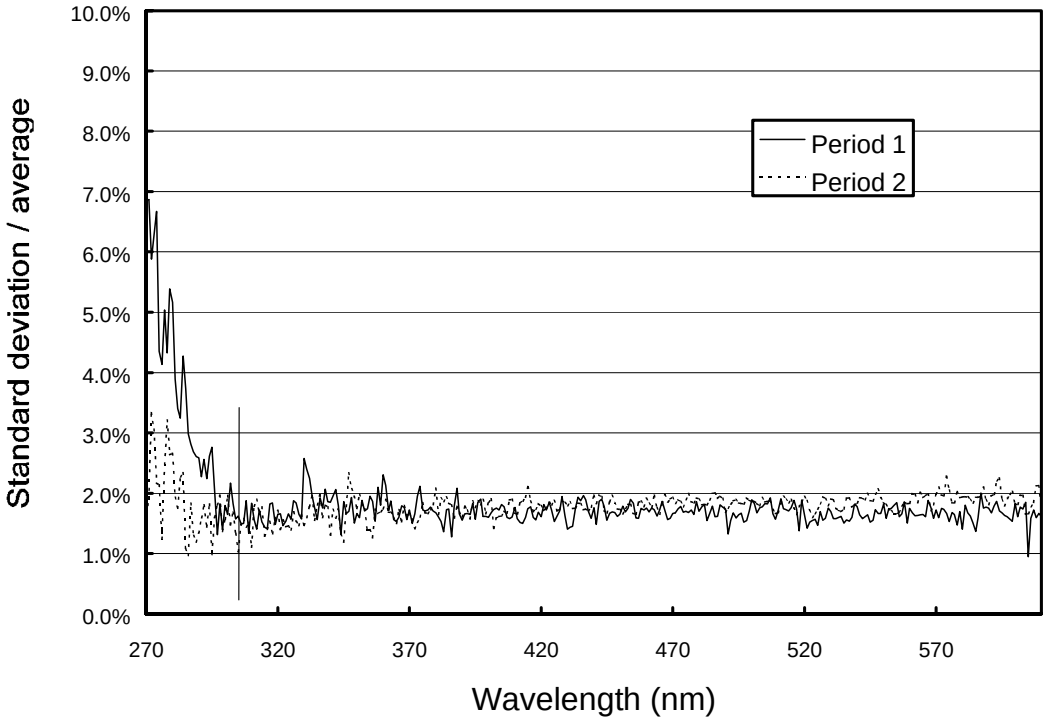

Figure 5.4.10. *Ratio of standard deviation and average calculated from the absolute calibration scans of Periods 1 and 2. The vertical line marks 305 nm, which is the cut-off wavelength of Period 1 data.*

.

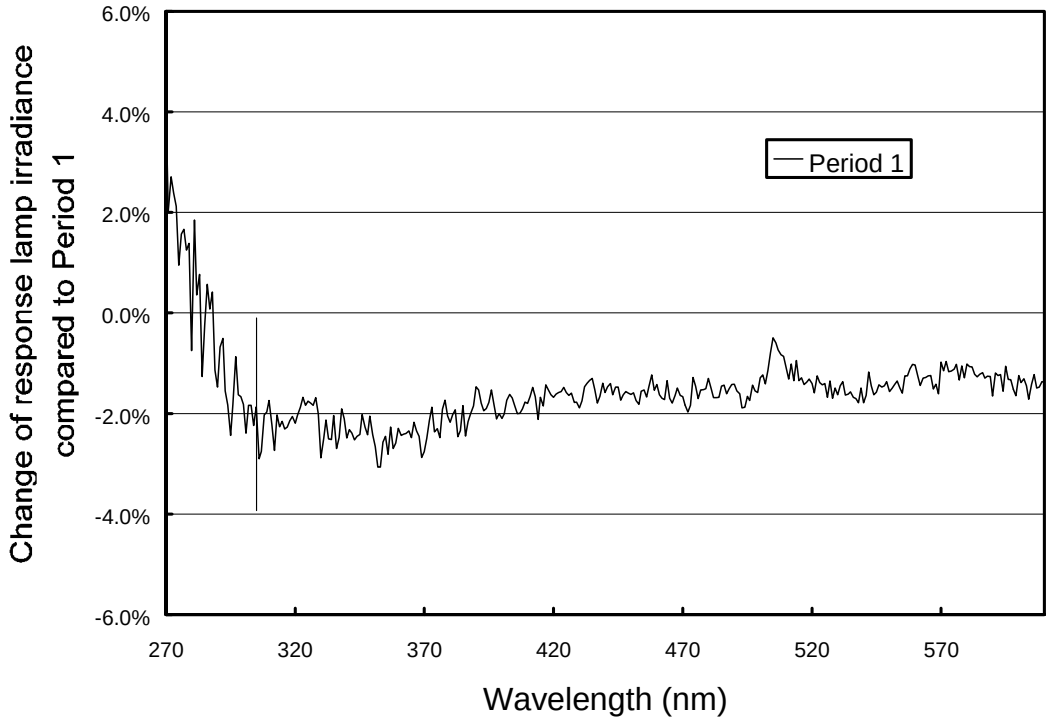

Figure 5.4.11. *Change of the response lamp's "mean irradiance" between Periods 1 and 2. The vertical line marks 305 nm, which is the cut-off wavelength of Period 1 data.*

5.4.3.4. Lamp Intercomparison

The site standards for the Volume 7 South Pole season were the lamps M-763, M-666, and 200W006. As for the other sites, M-874 served as a traveling standard. Lamp M-666 is a site spare without calibration. Since the lamp also appeared to have drifted over the season it was not used in the final instrument calibrations. M-763 was also one of the calibration lamps used during the last seasons at South Pole. It has a calibration from Optronics Laboratories from October 1992, which has been applied in previous years. For the current season, a new calibration has been transferred to the lamp, based on comparison with the traveling standard M-874. As mentioned earlier, several calibrations exist for M-874. We chose the calibration established by Optronic Laboratories in September 1995, which appeared to be the most appropriate for the time of the transfer. The "old" 1992 calibration and the "new" M-874-based calibration of M-763 deviate by about 4%. In the following, the change in the irradiance scale of M-763 is described in detail.

Figure 5.4.12 shows a comparison of the lamps M-763 and 200W006 with the traveling standard M-874 at the end of the season (1/4/98). Optronic Laboratories established the calibration of M-874 in 1995. The calibration of M-763 was transferred from M-874 using the 1995 calibration. For this transfer, absolute scans with both lamps preformed at the end of the season were evaluated. The very good agreement between M-874 and M-763 can therefore be expected and demonstrates the accuracy of the transfer procedure. Optronic Laboratories calibrated lamp 200W006 in 1996. The calibration deviates by about 1-2% from M-874.

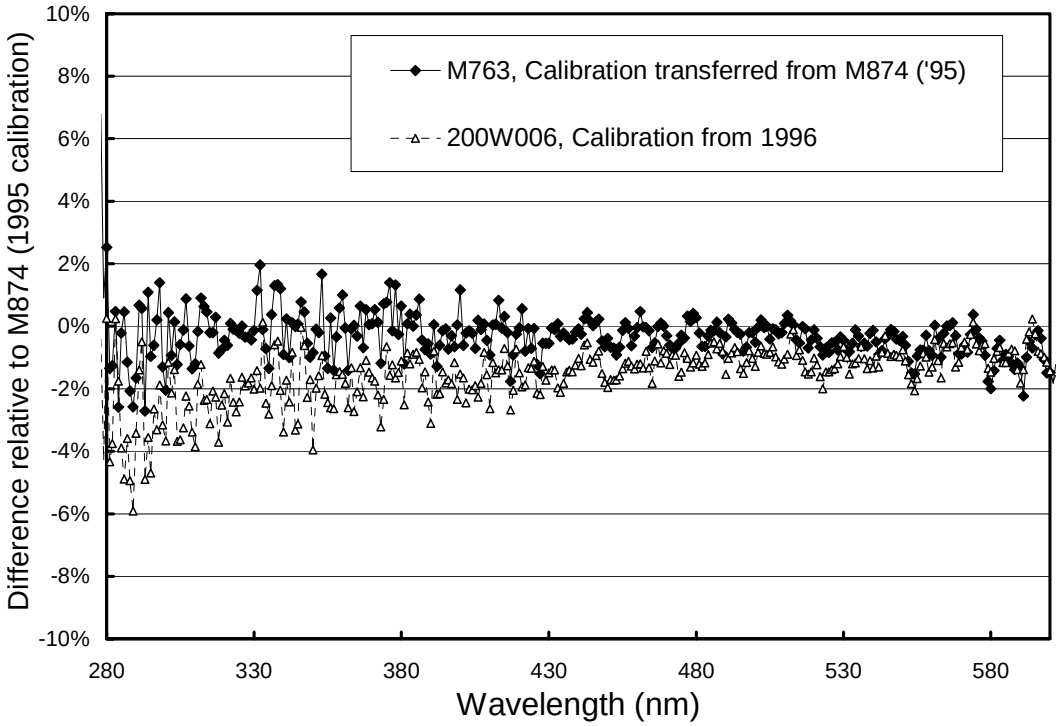

Figure 5.4.12. *Season closing calibrations; Comparison of the South Pole lamps M-763 and 200W006 with the traveling standard M-874 at the end of the season (1/4/98). Optronic Laboratories established the calibration of M-874 in 1995. The calibration of M-763 was transferred from M-874, and Optronic Laboratories calibrated 200W006 in 1996.*

Figure 5.4.13 shows the same absolute scans as were depicted in Figure 5.4.12. The calibration of M-763, however, is based on the Optronic Laboratories calibration from 1992 rather than derived by transfer from M-874. By comparing both figures, one can see that both calibrations of M-763 deviate by about 4%, almost independent of wavelength. This observation may have consequences when time-series of South Pole data from several seasons are compared. Since the calibration for a given season is based on more than one calibration standard—M-763 with the 1992 Optronic Laboratories calibration and lamp BSI201 were used for Volume 6, and M-763 with the M-874-based calibration and lamp 200W006 were used for Volume 7—the effect on time-series is only about 2%.

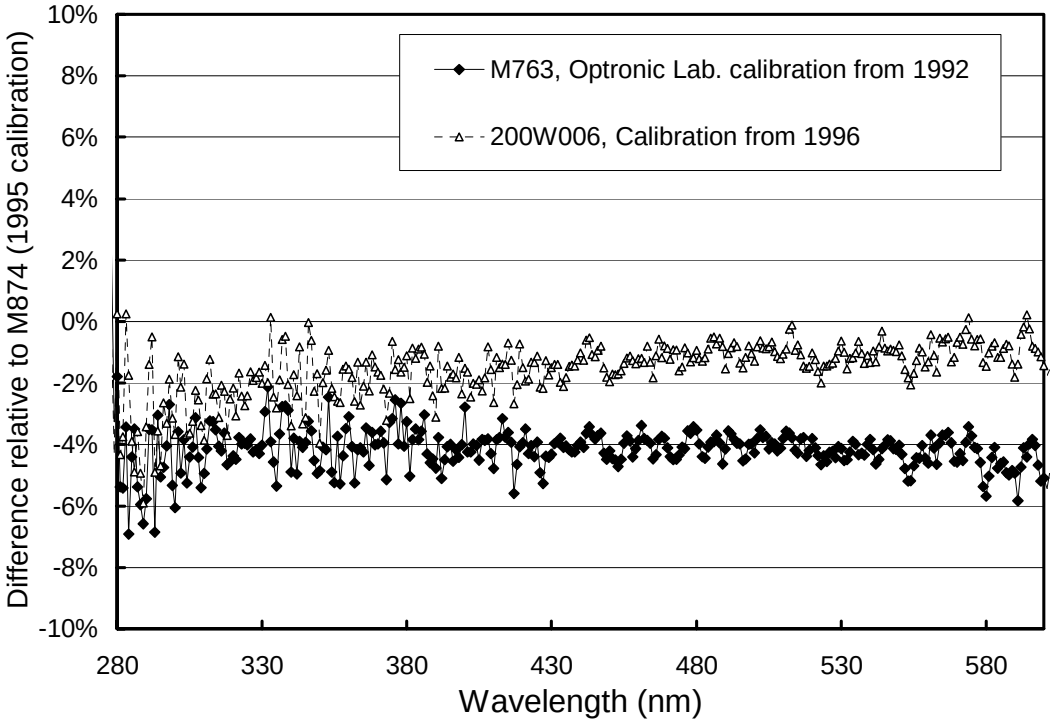

Figure 5.4.13. *Same as previous figure, except the calibration of M-763, which was established by Optronic Laboratories in 1992 rather than derived by transfer from M-874.*

Finally, Figure 5.4.14 shows a comparison of all lamps at the beginning of the season. The calibration of M-763 is based on the transfer from M-874. The plot is very similar to Figure 5.4.12 for wavelengths above 300 nm, confirming that all three lamps did not drift more than 1% during the season.

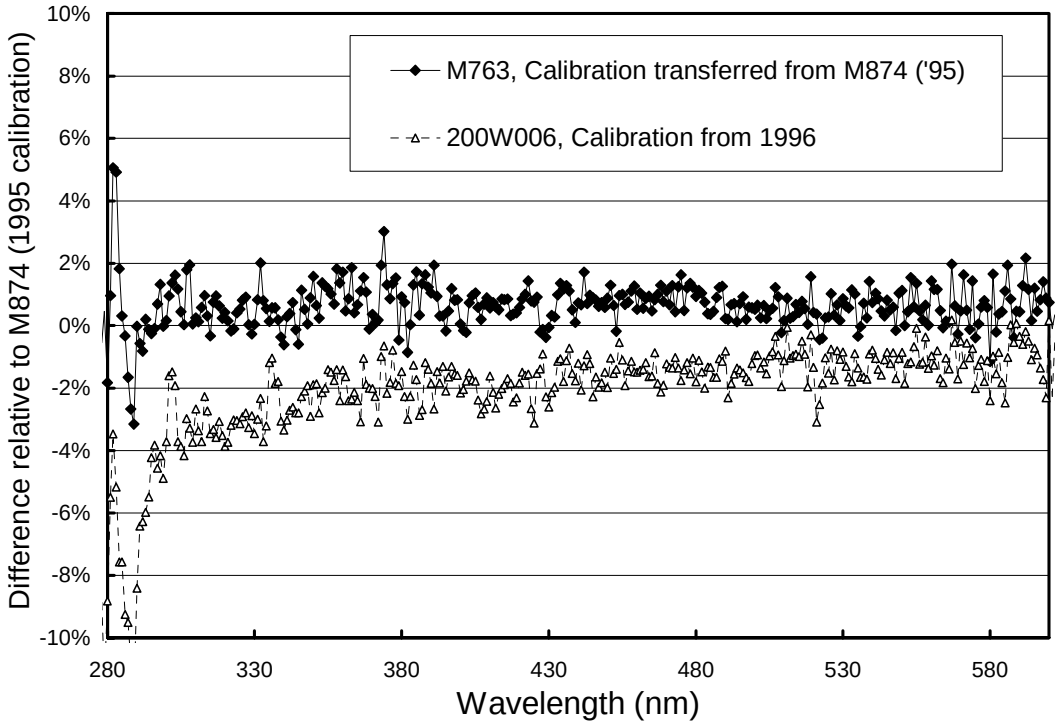

Figure 5.4.14. *Season opening calibrations; comparison of the South Pole lamps M-763 and 200W006 with the traveling standard M-874 at the beginning of the season (1/27/97). The calibration of M-874 was established by Optronic Laboratories in 1998. The calibration of M-763 was transferred from M-874 and 200W006 was calibrated by Optronic Laboratories in 1996.*

5.4.3.5. Azimuth Dependency of Volume 7 Data

As mentioned in the introduction to Section 5.4.3, we believe that the system's optics block consisting of diffuser, response lamp, wavelength standard, and beam splitters, became misaligned during the relocation of the system from the old Clean Air Facility to the new Atmospheric Research Observatory. Solar data therefore show a significantly higher azimuth dependency than in previous seasons. Although the actual reason for the problem has not yet been identified, we anticipate that the system does not exactly image the center of the diffuser on the monochromator's entrance slit. Another explanation could be that the inner part of the diffuser became tilted versus the outer ring, which serves as the reference plane for leveling. Since the solar zenith angle at South Pole is fairly constant during a day, the azimuth dependence appears as a sinusoidal wiggle in the data with a periodicity of one day.

Figure 5.4.15 demonstrates the azimuth dependence in solar spectral irradiance data. The effect is most pronounced at long wavelengths. At 600 nm, the wiggles have an amplitude of about ±10% of the daily average. At 320 nm, the variation almost disappears and is almost completely masked by variations due to clouds. The difference can be explained by the fact that radiation at 320 nm is mostly diffuse with only a small contribution from the direct sun. The position of the sun therefore only has a small influence. In contrast, radiation at 600 nm comes almost directly from the sun.

In Figure 5.4.16, time-series of spectral irradiance at 380 nm are compared with measurements of total irradiance, measured with the PSP, and readings of the TSI sensor. The period depicted is the same as in Figure 5.4.15. The measurements at 380 nm show less diurnal fluctuations than measurements at 600 nm, as can be expected. The center wavelength of the TSI is about 370 nm. The amplitude of the variations in the spectral measurements at 380 nm should therefore be comparable to the amplitude in the TSI readings. Figure 5.4.16 shows however that the TSI variation is only half of the variation that is apparent in the

spectral data. This, and the fact that both curves are not in phase, is a further indication that the optics were misaligned.

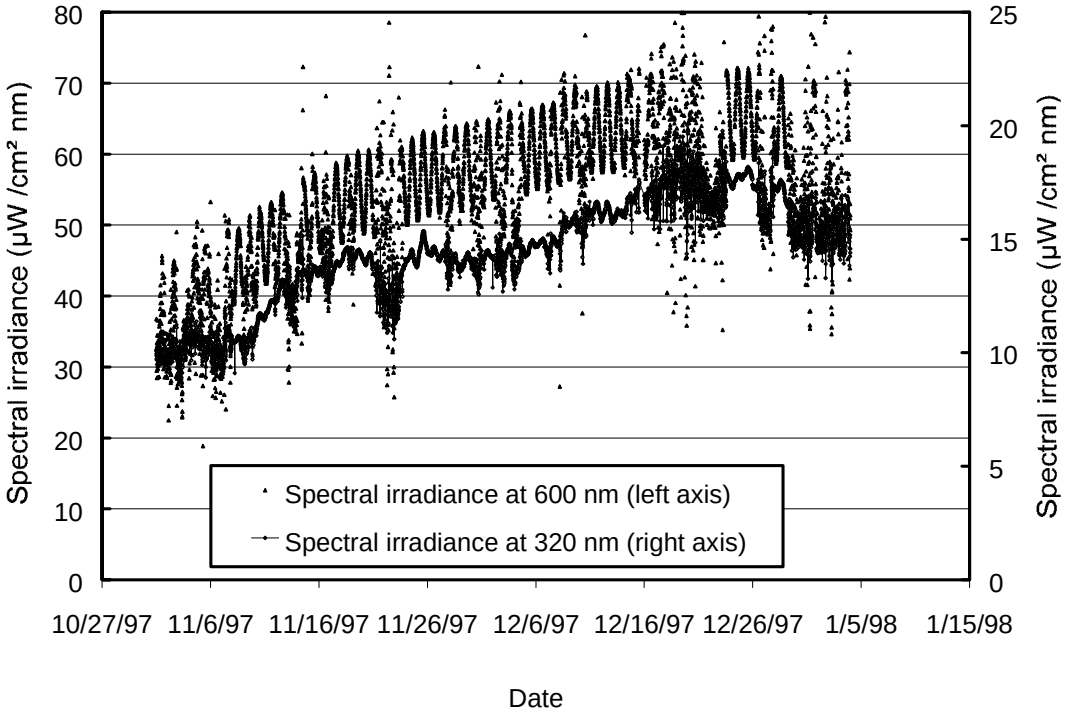

Figure 5.4.15. *Spectral irradiance at 320 and 600 nm measured at South Pole during November and December 1997.*

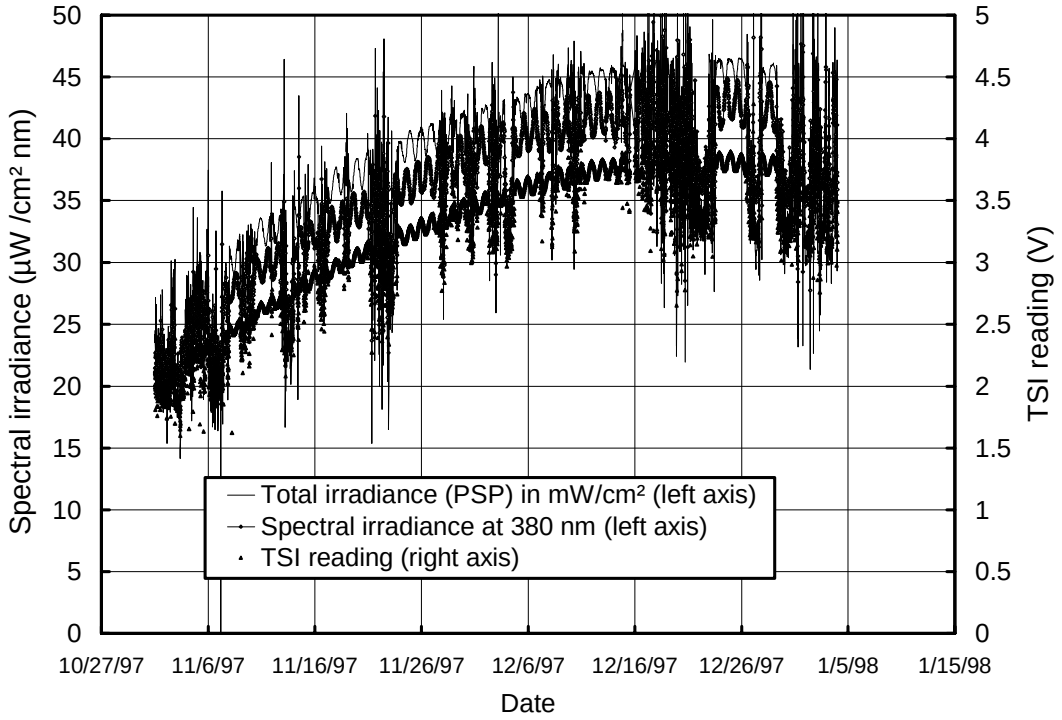

Figure 5.4.16. *Comparison of total irradiance measured by the PSP (highest curve), spectral irradiance at 380 nm (middle curve), and TSI reading (lowest curve).*

Also note that the PSP readings show a diurnal variations of about ±5%. This is surprising because the PSP is a completely independent instrument, which is not linked to the spectroradiometer's foreoptics. This indicates that the PSP may also be affected by azimuthal errors or that it was not correctly leveled. (Because of the high solar zenith angles prevailing at South Pole, small leveling errors may cause significant effects.) Although unlikely, a part of the asymmetry could also be caused by a directional dependence of ground reflection (albedo), which can be caused by snow snowdrifts (sastrugi).

From Figure 5.4.15 and Figure 5.4.16 it can be concluded that UV data are affected by the azimuth asymmetry by up to ±7%. At shorter UV-A wavelengths or at wavelength in the UV-B the asymmetry diminishes or almost disappears. The accuracy of daily averages or daily doses is only slightly reduced, because most of the systematic errors cancel out if measurements are integrated over one day.

5.4.3.6. Missing Data

A total of 13585 scans with SZA smaller than 92° were scheduled to be measured in the South Pole Volume 7 season. This is a substantial increase compared to previous seasons. This enhancement is the result of a change in the scan schedule after Polar Night, from 2 scans per hour to 4 scans per hour. 11769 scans, 86.6% of the scans scheduled, were actually measured, and 11230 scans (82.7%) are included in Volume 7.

A total of 3920 scans (28.9% of all scans scheduled) were affected by the electronic offset problem (see Section 5.4.3.1.). These scans were not excluded from the published data set, although columns with obviously wrong results were excluded until day 10/15/97.

- In Database 2, the entries in the fields E285_A, E285_C, E290, E295, E297, E298, E299, E300, E302_5 were deleted. The expression "Offset_problem" was stored in the field "Abnormal."
- In Database 3, the integrals E289_855to294_118, E294_118to298_507, E298_507to303_03 as well as the dose-weighted irradiances Dose1, Dose2, Setlow, Hunter, and Caldwell were deleted. The expression "Offset_problem" was stored in the field "Abnormal."
- In database 4, the dose-weighted irradiances Setlow, Hunter, and Caldwell were deleted.
- In the composite scans, spectral irradiance was set at zero for wavelengths below 303 nm.

The discrepancy of 1816 scans between scheduled and measured data scans has several reasons:

- Roughly 60 scans were superseded by absolute scans.
- 116 scans between 2/3/97 and 2/6/97 and 512 scans between 2/9/97 and 2/19/97 are missing because of hard disk failures
- In order to resolve system problems, an old DOS-based System Control software was installed between 2/21/97 and 3/6/97. With this software, measurements were performed in hourly rather than half-hourly intervals leading to a loss of 337 scans.
- Between 3/11/97 and 3/13/97 data scans were only measured hourly, causing a loss of 28 scans.
- Between 10/11/97 and 11/16/97 the problem with negative electronic offset was fixed. No scans were measured during these period; 513 scans were lost.

Not all scans measured are included in of Volume 7. Some scans were found to be defective and were therefore excluded from the final data set.

- On day 3/6/97 the new Windows NT®-based System Control software was installed again after the old DOS software was used for about 1.5 weeks. Problems with the configuration file caused defective wavelength, response, and data scans on the following days until the problem was solved on 3/11/97; 217 data scans were lost.
- The scans scheduled for 5:30 and 5:45 between 10/16/97 and 11/5/97 were shaded by a mast located close to the SUV-100; 38 scans were excluded.
- 21 scans on 10/23/97 appeared to be outliers and were excluded

- 42 scans had to be excluded on 10/15/97.